

## Light particle emissions in $^{12}\text{C} + ^{64}\text{Ni}$ at $E(^{12}\text{C}) = 35 - 70$ MeV

Zhang Li, Wang Da-yan, Jin Gen-ming, Zhang Bao-guo, and Wang Xi-ming  
*Institute of Modern Physics, Academia Sinica, Lanzhou, People's Republic of China*

(Received 1 August 1986)

Light particle emissions in the energy region slightly above the Coulomb barrier were studied. Energy spectra and angular distributions of p, d, t,  $^3\text{He}$ , and  $\alpha$  particles from the  $^{12}\text{C} + ^{64}\text{Ni}$  reaction were measured for the eight different incident energies below 70 MeV. The absolute cross sections and the contour plots of the Galilean-invariant cross sections  $d^2\sigma/pd\Omega dE$  are presented. The experimental proton energy spectra for  $E(^{12}\text{C}) \geq 50$  MeV have been well reproduced by the moving source model. This model includes two sources: a slow source moving at the velocity of the center of mass of the collision system, and a fast source moving at a velocity of about a half of the projectile velocity. The extracted source velocity and temperature parameters for the fast source were found to follow the previous systematic trend. The nonequilibrium components of some composite particles (d,  $^3\text{He}$ ,  $\alpha$ ), obtained by subtracting the relative equilibrium component from every measured spectrum, were accounted in terms of a generalized coalescence model.

### I. INTRODUCTION

Since the famous experiment was done by Britt and Quinton,<sup>1</sup> light particle emission in heavy-ion induced nuclear reactions has been extensively studied. With the earlier experimental results,<sup>1-3</sup> it has been confirmed that all light particle products may be divided into two parts: an equilibrium component evaporated statistically from the compound nuclei and a nonequilibrium component emitted from some fast nonequilibrium collision processes. In order to acquire new data and to explore the details of the reaction processes, many inclusive measurements,<sup>4-20</sup> as well as various correlation experiments,<sup>21-34</sup> were designed and completed. These studies showed that nonequilibrium emissions of light particles may occur at every stage prior to the attainment of full statistical equilibrium, such as quasielastic,<sup>3,11,35</sup> deep-inelastic,<sup>19,27,28</sup> incomplete fusion,<sup>15-18,21-26,30-32</sup> pre-equilibrium decay,<sup>4-12,20</sup> or sequential decay,<sup>28,29</sup> etc. A series of theoretical models has been developed, such as hot spot,<sup>36</sup> moving source,<sup>4-6</sup> coalescence,<sup>37,38</sup> exciton,<sup>39-41</sup> breakup,<sup>1,42</sup> and the sum rule model,<sup>26</sup> etc.

Up to now there have been only a few satisfactory experimental results<sup>8-15</sup> of light particle emissions at the low incident energy region near the Coulomb barrier except for  $\alpha$  particles.<sup>16-20</sup>

The cross sections of nonequilibrium components have been found to increase rapidly with projectile energy above the Coulomb barrier, especially for  $\alpha$ -particle emission. This implies that the reaction threshold energy of some nonequilibrium processes would be very low. So it seems to be predictable that there is a region of low bombarding energy in which the light particle emission mechanisms might be sensitive to both the projectile energy and the kind of the emitted light particle. Therefore, it is valuable to study the emission behavior of light particles in this region of incident energies.

The aim of this work is to provide a comprehensive set of data on light charged particle emissions in the in-

cident energies of 0.5-3 MeV per nucleon above the Coulomb barrier and to study how the emission mechanisms change and evolve with both the projectile energy and the kind of the outgoing particle. It would be interesting to examine if some successful models for higher incident energies are still appropriate at such low energies that have not been tested by other authors.<sup>4-6,10-12</sup> We chose the moving source model and the coalescence model for this purpose.

### II. EXPERIMENT

The experiment was performed at the 1.5 m Cyclotron of the Institute of Modern Physics, Lanzhou, China.  $^{12}\text{C}$  ion beams at eight different energies—69, 64, 56, 52.5, 49.5, 47.38, 46, and 35.8 MeV—were used.

The target was a 1.2 mg/cm<sup>2</sup>  $^{64}\text{Ni}$  isotope foil which was enriched to about 95%. Because a slight light-element contamination on the target will lead to an appendant cross section that should not be neglected, we paid much attention to preventing target contamination. The target was rolled up and stored carefully in an antiseptic vessel. In order to avoid target contamination from oil vapor during the measurement, an oil-free sputter ion pump system was used and a satisfactory vacuum  $5 \times 10^{-7}$  mm Hg was achieved. Moreover, several LN<sub>2</sub> refrigerating plates were set on the beam collimator or near the target. The whole target chamber system was separated from the accelerator vacuum system by using an Al foil in front of the collimator.

A counter telescope system consisting of three detectors,  $\Delta E1$ ,  $\Delta E2$ , and  $E$ , was used. The  $\Delta E1$  and  $\Delta E2$  were penetrable detectors of Au-Si surface-barrier type; their thicknesses are 38 and 94  $\mu\text{m}$ , respectively. The residual energy  $E$  detector was a Si(Li) type with a sensitive thickness of about 3 mm. The solid angle of the telescope was 0.54 msr. Clear identification for the five lightest ejectiles p, d, t,  $^3\text{He}$ , and  $\alpha$  particles was realized. Three energy signals from the three detectors were

recorded on a tape event by event. In an off-line analysis the energy spectra of various light particle products were derived from the data recorded on the tape. The recoil proton peaks formed by  $^{12}\text{C}$  ion beams on a mylar foil (with a thin carbon backing) were used as the calibration standard for proton spectra.

The  $\alpha$  particles emitted at the incident energies below 40 MeV and at backward angles for other energies were detected by a  $\Delta E-E$  semiconductor detector telescope comprising a  $14\ \mu\text{m}$   $\Delta E$  detector and an  $800\ \mu\text{m}$   $E$  detector.

The beam intensity was monitored by a Faraday cup. Integrated currents were used to normalize the data to obtain absolute cross sections. The experimental errors of differential cross sections are about 15% for p and  $\alpha$ , and 35% for d, t, and  $^3\text{He}$ .

### III. EXPERIMENTAL RESULTS

#### A. Energy spectra

Some energy spectra obtained at  $\theta_L = 15^\circ$  and  $25^\circ$  for proton and  $\alpha$  particle are shown in Fig. 1. They belong to six different beam energies from 69 to 47 MeV, respectively. These spectra have been transferred into the center-of-mass frame in order to make a comparison of the main characteristic between the two important products.

The first difference that can be seen in Fig. 1 is that the varying of the  $\alpha$ -particle's double differential cross section with the observation angle is more obvious than the proton's, especially as the incident energy is increased. The second difference is that the most probable

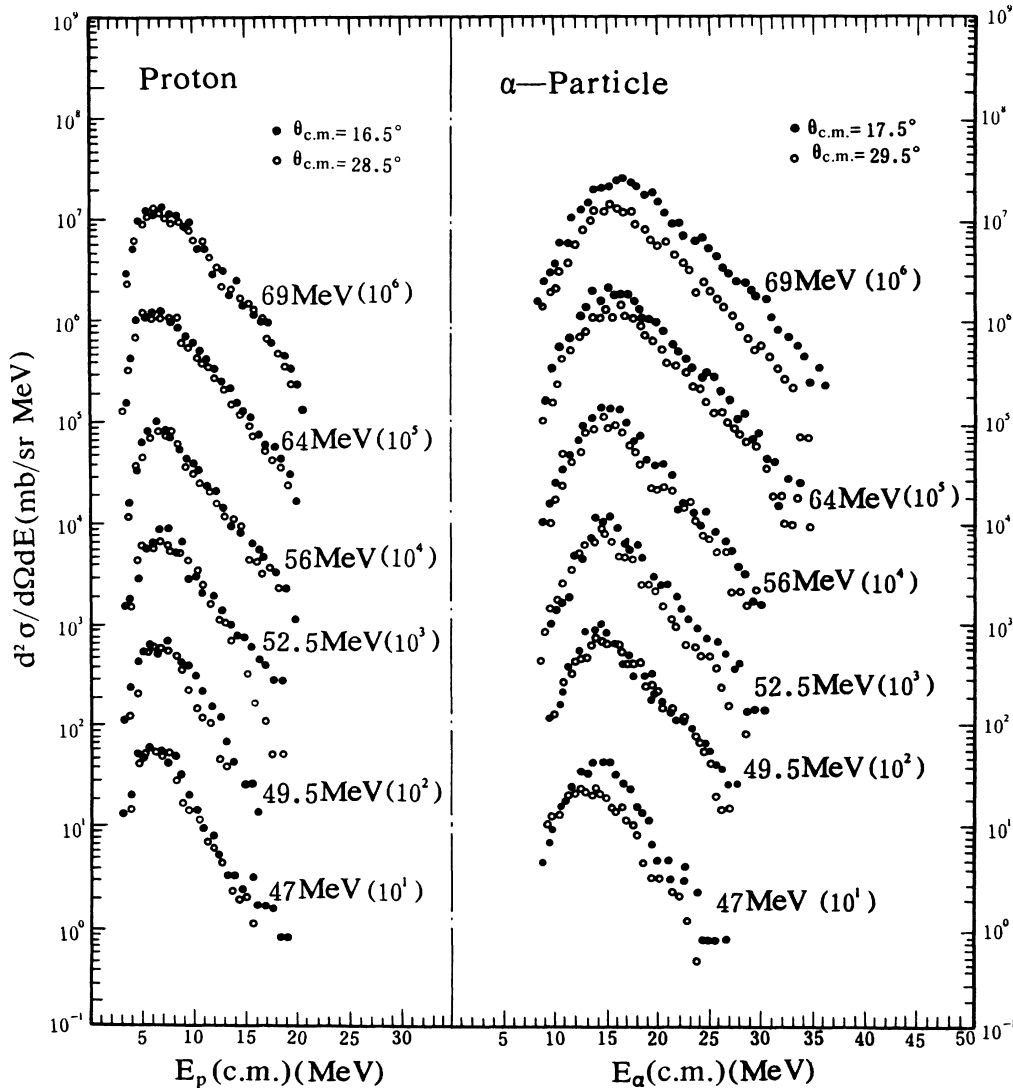


FIG. 1. Center-of-mass frame energy spectra of protons and  $\alpha$  particles in forward angles. The corresponding  $^{12}\text{C}$  beam energy of every set of the data are indicated in the figure.

energies (MPE) for proton spectra are not sensitive to either the incident beam energy or the observation angle. All of the proton MPE are within  $E_p = 6.5 \pm 0.7$  MeV, but the MPE of the  $\alpha$ -particle spectra clearly depend on both the projectile energy and observation angle. When reducing the incident beam energy from 69 to 35.8 MeV, the MPE of  $\alpha$  particle spectra at forward angles appear to vary from 16.8 to 11 MeV, in other words, from about beam velocity energy down to the Coulomb barrier for  $\alpha$  exit channel. At backward angles the MPE of  $\alpha$ -particle spectra are slightly above the Coulomb barrier for all eight beam energies.

The proton energy spectra are more asymmetrical than  $\alpha$ -particle ones. For example, for 69 MeV incident energy, the energetic tail of the proton spectra in the lab frame may extend to 4 times the beam velocity energy at forward angles. But the energy spectra of the  $\alpha$  particle only may extend to about 2.5 times the beam velocity energy at the same incident beam energy.

### B. Angular distributions

The angular distributions of p, d, t,  $^3\text{He}$ , and  $\alpha$  particles in the center of mass frame obtained at 69 and 56 MeV are shown in Fig. 2. The values of differential

cross sections are obtained by integrating the whole energy spectrum for every  $\theta_{c.m.}$  angle, respectively. All of these angular distributions are forward peaked with an increasing slope monotonically depending on the mass of the outgoing light particles. The proton angular distributions are rather smooth and the  $\alpha$ 's are very steep. In comparing the proton angular distributions with the  $\alpha$ -particle ones, it can be found that the differential cross sections are much lower for the proton than that for the  $\alpha$  particle at forward angles, but at backward angles the matter turns to the opposite. It implies a much larger equilibrium evaporation cross section for the proton than for the  $\alpha$  particle, and this fact is continued until the last 35.8 MeV incident energy.

When decreasing the projectile energy, the slopes of all angular distributions tend to decrease gradually. The proton angular distributions for below 50 MeV appear to be typically isotropic in which no structure may be seen. However, the varying of the  $\alpha$ -particle angular distributions are more complex as seen in Fig. 3. When the beam energies are reduced to 38.6 and 35.8 MeV, the angular distributions appear to peak at the angle approaching the grazing angle. The  $\theta_{gr}$  in Fig. 3 corresponds to the calculated grazing angles with the assumption of the nuclear radius parameter  $r_0 = 1.7$  fm.

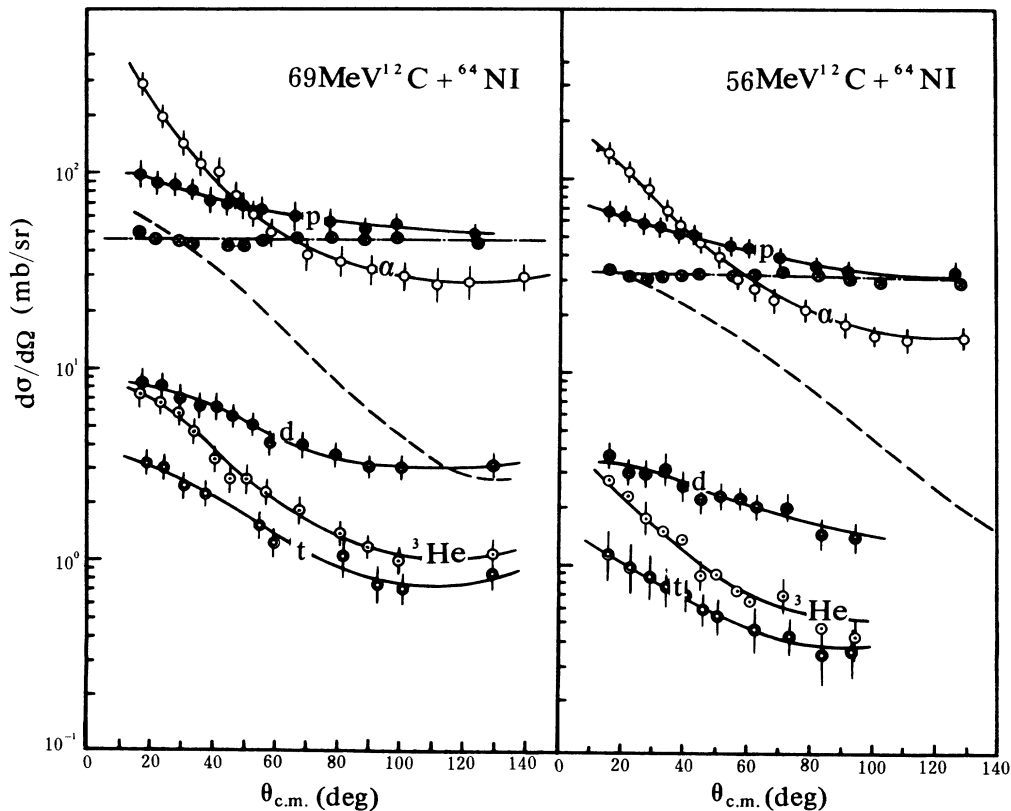


FIG. 2. The solid lines are the center-of-mass frame angular distributions obtained experimentally. The dashed lines are the angular distributions of the nonequilibrium proton emission calculated by the moving source model. The dotted and dashed lines show the difference between the experimental and the calculated values.

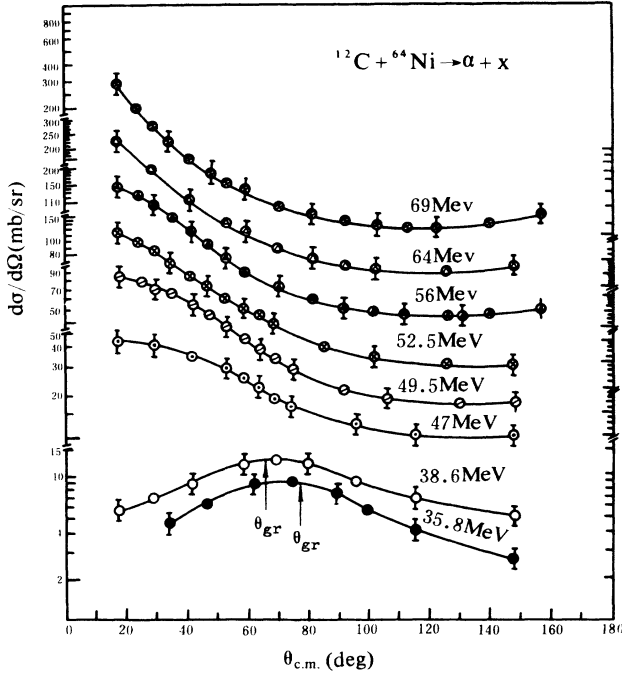


FIG. 3. The center-of-mass frame angular distributions of  $\alpha$  particles for eight  $^{12}\text{C}$  beam energies.

### C. Absolute cross sections and relative yields of the different isotopes

Total inclusive cross sections were obtained by integrating the angular distribution of every product p, d, t,  $^3\text{He}$ , and  $\alpha$  particles for eight different incident energies, respectively.

We tried to divide the total reaction cross sections into an equilibrium component  $\sigma_{\text{iso}}$  and a nonequilibrium component  $\sigma_{\text{non}}$ . The cross sections of the two com-

ponents for the  $\alpha$  particles were obtained by a universal method,<sup>1-3,8,16-19</sup> in which the angular distribution of the equilibrium component is assumed to be symmetrical with respect to  $\theta_{\text{c.m.}} = 90^\circ$ . For other composite particles d, t, and  $^3\text{He}$ , the same method as for  $\alpha$ 's was used. However, for the proton, besides the method as for  $\alpha$ 's, another method based on the moving source model calculation was used for getting the cross sections of nonequilibrium components. The details of this method are described in Sec. IV. The values of  $\sigma_{\text{iso}}$  and  $\sigma_{\text{non}}$  obtained by the methods described above are listed in Table I.

Average yield ratios between the different isotopes  $Y_p/Y_d$ ,  $Y_p/Y_t$ , and  $Y_\alpha/Y_{^3\text{He}}$  are shown in Fig. 4 as a function of projectile energy per nucleon above the Coulomb barrier  $(E - V_c)/A_p$ . Here  $V_c$  is calculated according to

$$V_c = \frac{(A_p + A_t)}{A_t} \frac{Z_p Z_t e^2}{r_0 (A_p^{1/3} + A_t^{1/3})}, \quad (1)$$

where  $A_p$ ,  $A_t$  and  $Z_p$ ,  $Z_t$  are the mass numbers and atomic numbers of the projectile and the target, respectively, and  $r_0 = 1.44$  fm. The ratios were calculated by the integration of yields over the angle range of  $15^\circ \leq \theta_L \leq 35^\circ$ . The part of the real yield below the integration threshold energies indicated in Fig. 4 have been cutoff in summing the yields.

All of these ratios measured at such low projectile energies display some anomalous structures that are hard to be understood.

In Fig. 4(a) a result obtained for 140 MeV  $^{16}\text{O}$  on  $^{197}\text{Au}$  by Awes *et al.*<sup>5</sup> is also shown together with the data of this work. Considering the fact that the value was given over a larger angle range, it might be thought to link up with the experimental points of this work although it is from a different reaction.

TABLE I. Total inclusive cross sections (mb) of light-charged particle products from the reaction of  $^{12}\text{C}$  ion on  $^{64}\text{Ni}$  target (absolute errors 15% for p and  $\alpha$ ; 35% for d, t, and  $^3\text{He}$ ).

$E(^{12}\text{C})$ MeV	Protons		Deuterons		Tritons		Helium-3			Alpha	
	iso	$\sigma$ non	iso	$\sigma$ non	iso	$\sigma$ non	iso	$\sigma$ non	iso	$\sigma$ non	
69	808	130 (172) <sup>a</sup>	33	15	9	6	13	11.3	397	360	
64	634	120 (145) <sup>a</sup>							338	318	
56	509	104 (119) <sup>a</sup>	18	6	4.5	1.4	4.5	4.4	234	248	
52.5	424	60 (78) <sup>a</sup>							182	199	
49	374	40 <sup>b</sup>							145	166	
47	330	30 <sup>b</sup>							123	112	
38.6	276								58	52	
35.8	201								34	38	

<sup>a</sup>Calculated values using the moving source model (see text).

<sup>b</sup>Estimated values.

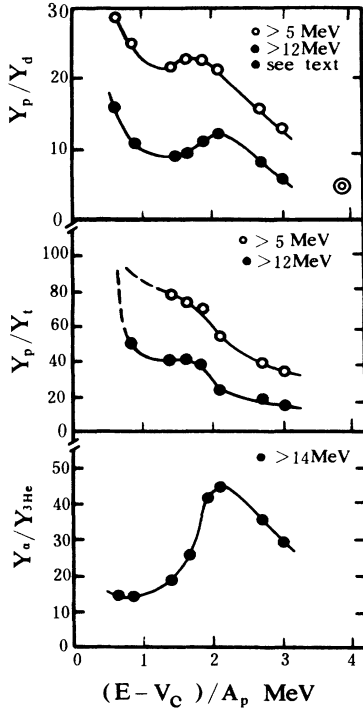


FIG. 4. The relative yield ratios of different H or He isotopes for the angle range  $15^\circ \leq \theta_L \leq 35^\circ$ . The  $\odot$  is given by Awes *et al.* (Ref. 5) for the  $^{16}\text{O} + ^{197}\text{Au}$  system for  $0^\circ < \theta_L < 180^\circ$ .

#### IV. ANALYSES

##### A. The contour plots of the Galileo-invariant cross section

In order to investigate whether the present data can be described by an isotropic evaporation from a moving thermal source, two typical contour plots of the Galileo-invariant cross section  $d^2\sigma/pd\Omega dE$  in the velocity plane are shown in Fig. 5. They were made for protons and  $\alpha$  particles at 69 MeV  $^{12}\text{C}$  beam energy.

In the proton contour plot the contour lines in the forward directions and those in the backward directions can be regarded as two sets of concentric arcs. Their common centers are located at  $v_{\parallel}/c = 0.037$  and  $v_{\parallel}/c = 0.018$ , respectively. Here  $c$  is the velocity of light.

But the contour lines in the forward directions of the  $\alpha$  particle contour plot cannot be regarded as a set of concentric arcs, because they do not have a common center. The smaller the observation angle is, the larger the curvature radius of the contour line. This implies that there could be a "third component" from the break-up of the  $^{12}\text{C}$  ion in the  $\alpha$  product which is emitted towards forward angles. The characters of contour lines at the backward angles in both cases of proton and  $\alpha$  particles are quite similar.

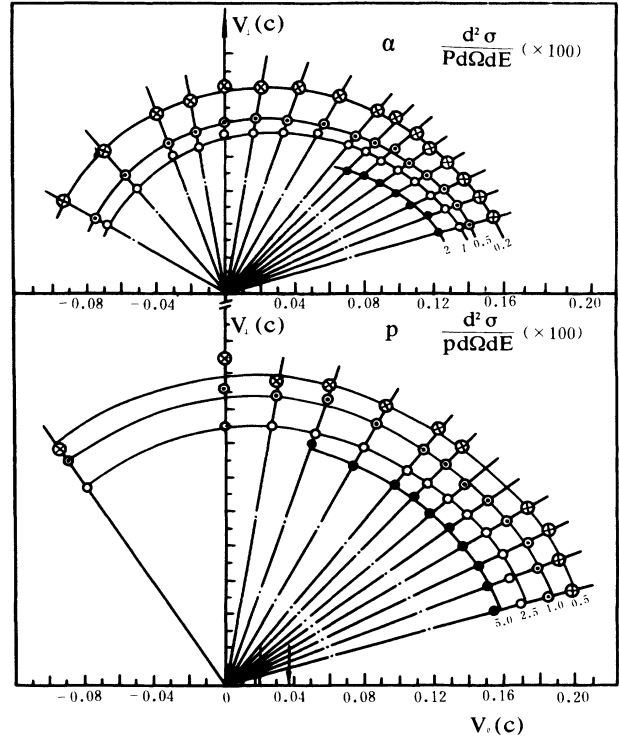


FIG. 5. The contour plots of Galileo-invariant cross sections in velocity plane for  $E(^{12}\text{C}) = 69$  MeV.  $V_{\parallel}$  and  $V_{\perp}$  are the parallel and perpendicular component of particle velocity, respectively, in unit of the light velocity.

The result of the  $\alpha$  particle presented here is different from that given by Borcea *et al.*<sup>11</sup> In Ref. 11 a similar plot for the  $\alpha$  product from the reaction  $^{181}\text{Ta} + ^{22}\text{Ne}$  (8 MeV/nucleon) was shown and the curvature centers of all contour lines at forward directions are almost exactly at the same position  $V_{\parallel} = 0.053c$ . This might have been caused by the differences of the reaction systems.

##### B. Moving source model

In the moving source model, light particles are assumed to be emitted isotropically from a source moving with an intermediate velocity between projectile and target nucleus velocities. It has been demonstrated to be valid for the beam energies above 7.5 MeV/nucleon.<sup>4-6,10-12</sup> In this study its validity at even lower energies was investigated.

The experimental proton energy spectra have been analyzed by the moving source model. Two different forms of the moving source model were used in our analysis.

In the single source form the expressions<sup>4-6</sup> are as follows:

$$\frac{d^2\sigma}{d\Omega dE} = N_0 f(v_s, T_s, E_C), \quad (2)$$

$$f(v_s, T_s, E_C) = (E - ZE_C)^{1/2} \exp\{-[E - ZE_C + E_1 - 2E_1^{1/2}(E - ZE_C)^{1/2} \cos\theta]/T_s\}. \quad (3)$$

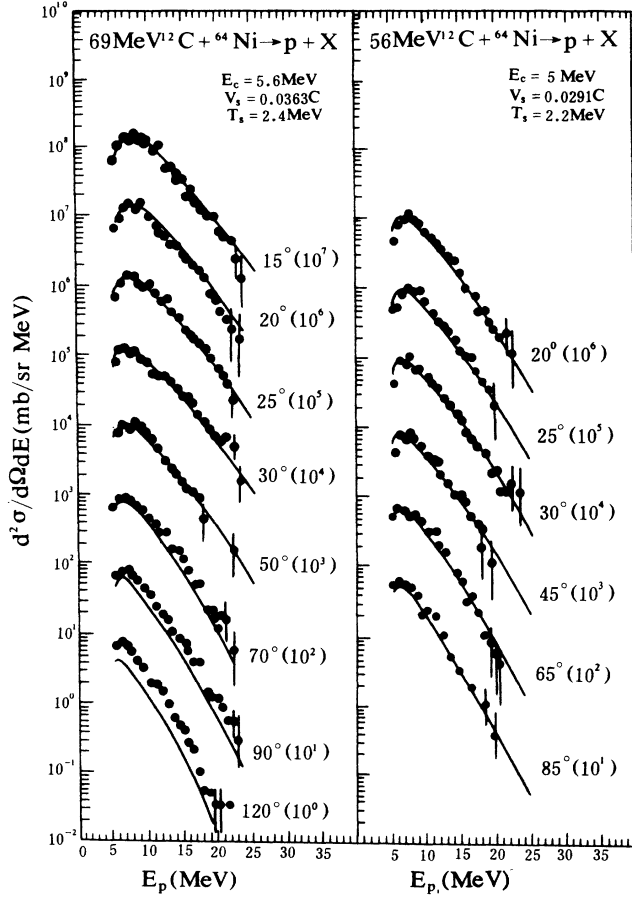


FIG. 6. The experimental proton energy spectra (dots) and the calculated ones (solid line) by the single source form of the moving source model.

Where  $E_1 = 1/2mv_s^2$  is the kinetic energy of a particle at rest in the moving frame, so  $v_s$  is the so-called source velocity.  $N_0$  is the overall normalization constant that may be understood as a probability relating to the formation and decay of the imaginary source.  $ZE_C$  is the Coulomb energy of a light particle with charge  $Ze$ ,  $T_s$  is the source temperature, and  $\theta$  is detection angle.

For the double source form we have<sup>6</sup>

$$\frac{d^2\sigma}{d\Omega dE} = N_{cn} f(v_{cn}, T_{cn}, E_{C,cn}) + N_p f(v_p, T_p, E_{C,p}), \quad (4)$$

where the subscript "cn" corresponds to the slow velocity source and "p" to the fast velocity source.

TABLE II. The parameters extracted by fitting the moving source model of the single source form to the proton spectra from  $^{12}\text{C} + ^{64}\text{Ni}$  reaction.

$E(^{12}\text{C})$ (MeV)	$v_s(c)^a$	$T_s$ (MeV)	$E_C$ (MeV)	$N$ [mb/(MeV) <sup>3/2</sup> sr]
69	0.0363	2.4	5.6	12.5
64	0.0345	2.3	5	11.4
56	0.0291	2.2	5	9.5
52	0.0265	2	5	9

<sup>a</sup>The unit  $c$  is the velocity of light.

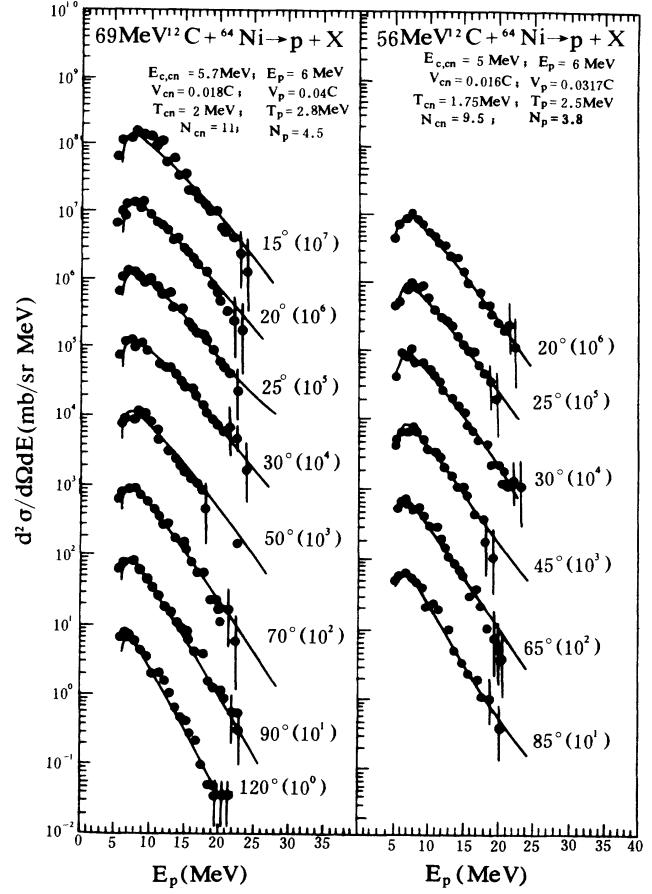


FIG. 7. The same as in Fig. 8, but the calculated spectra are obtained by the double source form.

The experimental proton energy spectra are compared with the calculated ones given by the single source form in Fig. 6. It can be seen that the proton spectra at forward angles are well reproduced by the single source form calculation, but at backward angles the experimental values of double differential cross sections are much higher than the calculated values. The parameters extracted from fitting the single source form to the proton energy spectra at four incident energies are listed in Table II. For the 69 MeV incident energy the optimum fitting source velocity  $v_s$  is 0.0363c which is consistent with the position of the center of proton contour lines at forward angles in Fig. 5. It also corresponds to a ratio of  $v_s/v_b = 0.45$ , here  $v_b$  is the projectile velocity after slowing down in the Coulomb field.

We have also made the fitting of the double source

TABLE III. The parameters extracted by fitting the moving source model of the double source form to the proton spectra of a same set as in Table II.

$E(^{12}\text{C})$ (MeV)	Center-of-mass velocity source				Faster velocity source			
	$v_{cn}$ (c) <sup>b</sup>	$T_{cn}$ (MeV)	$E_{C,cn}$ (MeV)	$N_{cn}$ <sup>a</sup>	$v_p$ (c) <sup>b</sup>	$T_p$ (MeV)	$E_{C,p}$ (MeV)	$N_p$ <sup>a</sup>
69	0.018	2	5.7	11	0.04	2.8	6	4.5
64	0.017	1.85	5	11	0.037	2.6	6	4.5
56	0.016	1.75	5	9.5	0.0317	2.5	6	3.8
52	0.0154	1.65	5	8	0.0289	2.2	6	2.8

<sup>a</sup>The units of  $N_{cn}$  and  $N_p$  are  $\text{mb}/[(\text{MeV})^{3/2}\text{sr}]$ .

<sup>b</sup>The unit  $c$  is the velocity of light.

form to the same set of proton spectra and the corresponding results are given in Fig. 7 and Table III. It can be seen that the double source form can improve the reproduction of the spectra of the backward angles.

In Fig. 8 the extracted source velocities and source temperatures corresponding to the fast source have been included in the figure given by Awes *et al.*<sup>5</sup> In Fig. 8 the velocities and temperatures of the moving source ex-

tracted from various reaction systems appear to have an almost linear dependence on the projectile velocity after slowing down in the Coulomb field. It is obvious that those parameter values presented by this study follow well the systematic trend and can link up with earlier experimental points towards low energy direction.

In the moving source model, angular distributions can also be calculated by an expression as follows:<sup>5</sup>

$$\frac{d\sigma}{d\Omega} = \frac{N_0}{2\pi} (\pi T)^{3/2} e^{-E_1 \sin^2\theta/T} \left\{ (1+2x^2) + \left[ (1+2x^2)\text{erf}(x-y) + \frac{2}{\pi^{1/2}}(x+y)e^{-(x-y)^2} \right] \right\}, \quad (5)$$

where  $E_1 = \frac{1}{2}mv^2$ ,  $x = (E_1/T)^{1/2}\cos\theta$ , and  $Y = [(E_T - E_C)/T]^{1/2}$ .  $v$ ,  $T$ ,  $E_C$ , and  $N_0$  are the moving source model parameters that have been determined by fitting the model to the proton spectra.  $E_T$  is the low energy threshold for integrating the energy spectra.

The calculated proton angular distributions that have been transferred to the center of mass frame for the 69 and 56 MeV beam energies are shown by the dashed curves in Fig. 2. They correspond to the contributions from the faster source in the double source form. So the relative parameters  $v_p$ ,  $T_p$ ,  $E_{C,p}$ , and  $N_p$  have been used, and  $E_T = 6.5$  MeV. The distributions of the differences between the experimental differential cross sections of protons and the calculated ones are also shown in Fig. 2. These differences can be found to be typical isotropic distributions. Thus we can divide the total experimental cross section into an equilibrium component and a non-equilibrium component by means of the moving source model calculations. The cross sections of nonequilibrium proton emission obtained by integrating the calculated angular distributions are given in Table I together with the values derived directly from the experimental angular distributions.

The same fitting as for the protons was also done for  $\alpha$  particles; however it failed. We cannot find a set of parameters to reproduce simultaneously the  $\alpha$ 's spectra of different angles. Therefore, the moving source model might not be appropriate for the description of the emission process of  $\alpha$  particles. The failure might be caused by the existence of a "third" source relating to the "third" component that has been discussed above.

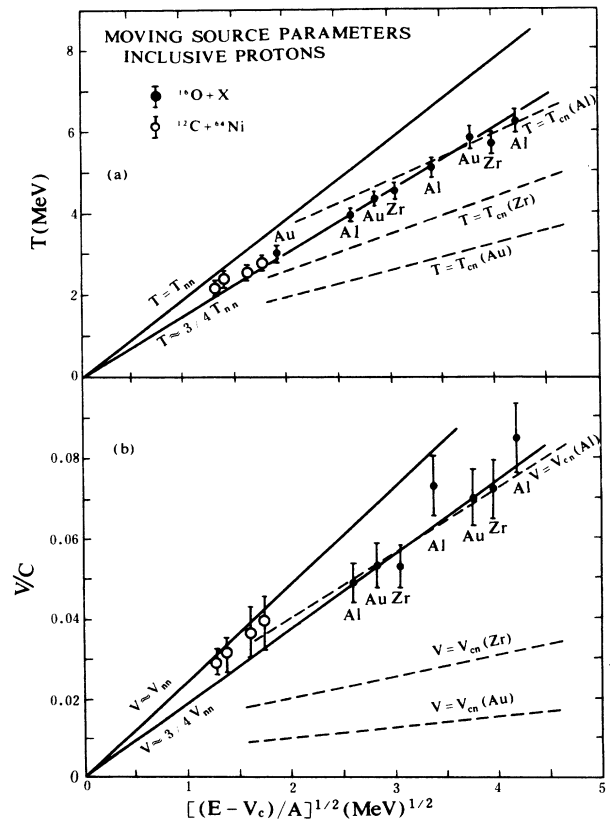


FIG. 8. Incident energy and target dependence of the moving source temperature and velocity parameters given by Awes *et al.* (Ref. 5). For comparison the results obtained from this work for  $^{12}\text{C} + ^{64}\text{Ni}$  are shown by open circles.

### C. Coalescence model

In the coalescence model<sup>5,6,37</sup> the coalescence relation is explained by the assumption that composite particles are formed by the coalescence of free nucleons which happen to occupy the same region of momentum space.<sup>43,44</sup> The model is a pure phase space approach and makes no assumption about the dynamics of the reaction. It involves a single free parameter, the coalescence radius  $P_0$ , which is the radius of the sphere in momentum space within which the coalescence occurs.

Recently, the coalescence relation had been demonstrated to be valid for bombarding energies down to 10 MeV/nucleon.<sup>5,10</sup> In this work the validity of the coalescence model has been investigated for the incident energies of about 5 MeV/nucleon. We used a generalized coalescence model<sup>5,6</sup> which takes Coulomb repulsion from the target nucleus into account. The differential multiplicity  $d^2M(Z, N, E)/dE_A d\Omega$  of composite particles consisting of  $Z$  protons and  $N = A - Z$  neutrons with energy  $E$  is related to that for protons,  $d^2M(1, 0, E)/dE d\Omega$ , as follows:

$$\begin{aligned} \frac{d^2M(Z, N, E_A)}{dE_A d\Omega} &= \left[ \frac{N_t + N_p}{Z_t + Z_p} \right]^N \\ &\times \frac{A^{-1}}{N!Z!} \left[ \frac{4/3P_0^3}{[2m_0^3(E - E_C)]^{1/2}} \right]^{A-1} \\ &\times \left[ \frac{d^2M(1, 0, E)}{dE d\Omega} \right]^A, \end{aligned} \quad (6)$$

where  $E_A = AE - NE_C$  and  $E_C$  is the Coulomb repulsion per unit charge.  $N_t$ ,  $N_p$  and  $Z_t$ ,  $Z_p$  are the neutron and proton numbers of target and projectile, respectively, and  $m_0$  is the nucleon rest mass. Here it is assumed that the energy distributions of the coalescing protons and neutrons have the correlation,

$$\frac{d^2M(0, 1, E)}{dE d\Omega} = \frac{N_t + N_p}{Z_t + Z_p} = \frac{d^2M(1, 0, E + E_C)}{dE d\Omega}, \quad (7)$$

although this assumption may not be completely valid.<sup>45</sup> The differential multiplicity is related to the corresponding cross section as follows:<sup>37</sup>

$$\frac{d^2M(Z, N, E_A)}{dE_A d\Omega} = \frac{1}{\sigma_0} \frac{d^2\sigma(Z, N, E_A)}{dE_A d\Omega}, \quad (8)$$

where  $\sigma_0$  is usually approximated by the total reaction cross section and  $\sigma_R$  is calculated by the expression

$$\sigma_R = \pi[r_0(A_p^{1/3} + A_t^{1/3})]^2(1 - V_B/E_{c.m.}), \quad (9)$$

where  $E_{c.m.}$  is the center-of-mass frame kinetic energy of the incident ion and  $V_B$  is the Coulomb barrier of the entrance channel. Here let  $r_0 = 1.5$  fm.

At low incident energies, the evaporation cross section from compound nuclei constitutes a large fraction of the total cross section of light particle emission. As mentioned in Sec. III, the cross sections of equilibrium evaporation component for the proton are much larger than those for the  $\alpha$  particle. Therefore it might be expected

that fitting Eqs. (6)–(9) to the composite particle spectra will come to a failure at low beam energies if we use directly the measured proton spectra. In view of this problem, Fukuda *et al.*<sup>10</sup> used the proton spectra derived from the measured deuteron particle energy spectra in order to reduce the contribution from the equilibrium emission. They achieved good agreement for t and  $\alpha$  particle spectra, but the value of  $E_C = 3$  MeV that was used in their calculation is much lower than the reasonable values of  $E_C = 5$ –6 MeV. In this work we obtained the proton spectra that will enter into the coalescence calculation by means of a new method. We have proved in Sec. IV B that the moving source model with two sources provides a way to divide the light particle products into two components, an equilibrium and a non-equilibrium. In terms of Eqs. (2) and (3), as well as the parameters  $v_p$ ,  $T_p$ ,  $N_p$ , and  $E_{C,p}$ , we obtained the expectant proton spectra. The corresponding composite particle spectra were obtained by subtracting the contributions of equilibrium evaporation from each measured energy spectra, respectively.

Some comparisons of the experimental energy spectra with the calculated spectra obtained in this way are shown in Fig. 9. Here we used a value of  $E_C = 6$  MeV. Extracted coalescence radii in momentum space are 190, 118, and 65 MeV/c for  $\alpha$ ,  ${}^3\text{He}$ , and d, respectively, at 69 MeV and 205 MeV/c for  $\alpha$  at 56 MeV. Generally, the agreement is quite successful, however it was found for the  $\alpha$ -particle spectra at the most forward angles that there are some superfluous cross sections in the vicinity of the beam velocity energy which cannot be interpreted by the coalescence model calculation. It is also an evidence of the existence of the so called “third component” in the  $\alpha$  product.

### V. SUMMARY

We have studied the emission behavior of light-charged particles p, d, t,  ${}^3\text{He}$ , and  $\alpha$  in the  ${}^{12}\text{C}$  induced reaction on  ${}^{64}\text{Ni}$  target at the incident energies of 0.5–3 MeV/nucleon above the Coulomb barrier.

The direct evidence of nonequilibrium emission of protons in this energy region has been obtained from the analysis of the contour plot of the Galileo-invariant proton cross sections. The moving source model involving two sources is found to be quite successful in reproducing the proton energy spectra at all angles. The extracted velocity and temperature parameters relating to the fast source follow the systematic trend given by Awes.<sup>5</sup> The source velocities of the fast source are about one-half of the beam velocity after slowing down in the Coulomb field. It was also demonstrated that the entire proton product can be divided into an equilibrium component and a nonequilibrium component in terms of the double source model calculation.

The validity of the coalescence model in this energy region was also studied. The energy spectra of the composite particles  $\alpha$ , d, and  ${}^3\text{He}$  after excluding the contribution of equilibrium evaporation have been reproduced by the coalescence relation calculation. Here the proton spectra were calculated by the moving source model ac-

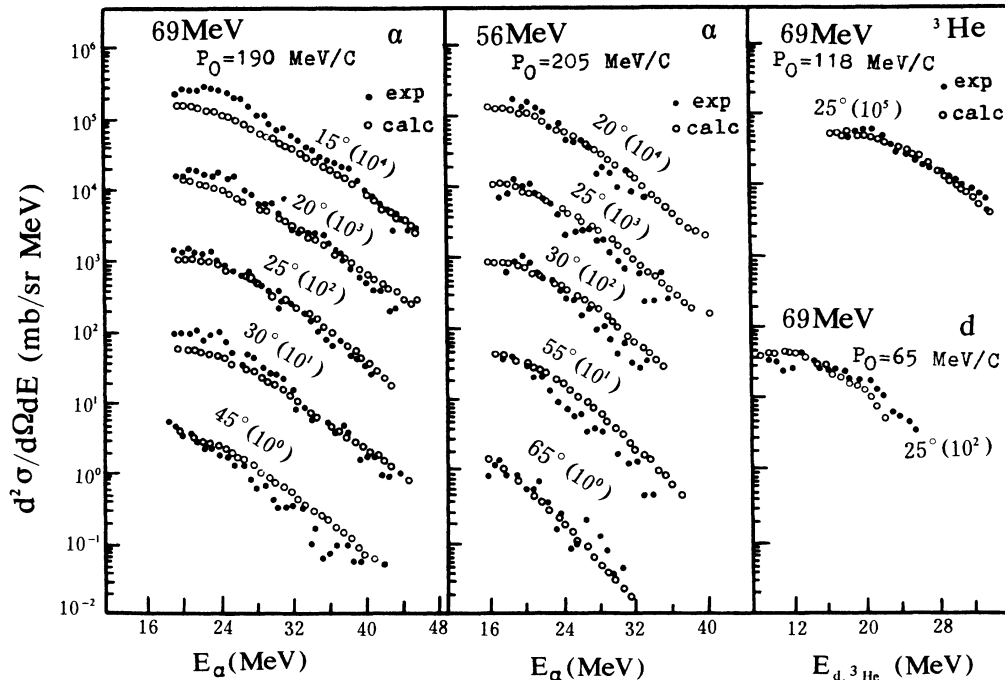


FIG. 9. The experimental composite particle spectra after excluding the contribution from equilibrium evaporation and the calculated spectra by the coalescence model.

cording to the method described in Sec. IV C. We infer that the coalescence relation may be valid only in the preequilibrium emission process and it is still an appropriate model for bombarding energy down to 2–3 MeV/nucleon above the Coulomb barrier.

The experimental results and model analyses indicate that the threshold for nonequilibrium proton emission corresponds to a projectile energy of about 1.5 MeV/nucleon above the Coulomb barrier. However for  $\alpha$ -particle emissions, the nonequilibrium component can still be seen down to a projectile energy just above the Coulomb barrier. The only nonequilibrium process for proton emissions seems to be preequilibrium emission in this energy region; however, the variations of the emission mechanism for  $\alpha$  particles are quite complex. The quasielastic massive transfer may occur from the incident energy just above the Coulomb barrier. For an energy of about 1 MeV/nucleon above the Coulomb bar-

rier, the preequilibrium emission and deep inelastic collision transfer may be possible. When the incident beam energy increases to the value of 2.5 MeV/nucleon above the Coulomb barrier, the so called “third source” produced from the breakup of  $^{12}\text{C}$  projectiles might emerge. Some evidence for the breakup process has been obtained from the data analyses.

#### ACKNOWLEDGMENTS

We would like to thank Prof. Yang Cheng-zhou, Prof. Dai Guang-xi, and Prof. Zhu Yong-tai for many stimulating discussions concerning the interpretation of the present experimental results. We wish to extend our appreciation to Prof. Zheng Ji-wen for frequent help and encouragement. Mr. W. Jackson, Mrs. C. Jackson, Dr. Lin Bing, and Prof. Liu Guo-xing gave us much help during the writing of this paper.

<sup>1</sup>H. C. Britt and A. R. Quinon, *Phys. Rev.* **124**, 877 (1961).

<sup>2</sup>J. Galin, B. Gatty, D. Guerreau, C. Rousset, U. C. Schlotthauer-Voos, and X. Tarrago, *Phys. Rev. C* **9**, 1126 (1974).

<sup>3</sup>Shen Wen-qing, Xu Shu-wei, Wang Da-yan, Sie Yuan-xiang, Guo Zhong-yan, and Li Zu-yu, *Phys. Energ. Fort. Phys. Nucl.* **1**, 70 (1977).

<sup>4</sup>T. J. M. Symons, P. Doll, M. Bini, D. L. Hendrie, J. Mahoney, G. Mantzouranis, D. K. Scott, K. Van Bibber, Y. P. Viyegi, H. H. Wieman, and C. K. Gelbke, *Phys. Lett.* **B94**, 131 (1980).

<sup>5</sup>T. C. Awes, S. Saini, G. Poggi, C. K. Gelbke, D. Cha, R. Legrain, and G. D. Westfall, *Phys. Rev. C* **25**, 2361 (1982).

<sup>6</sup>T. C. Awes, G. Poggi, C. K. Gelbke, B. B. Back, B. G. Glagola, H. Breuer, and V. E. Viola, Jr., *Phys. Rev. C* **24**, 89 (1981).

<sup>7</sup>D. Logan, H. Delagrange, M. F. Rivet, M. Rajagopalan, John M. Alexander, Morton Kaplan, M. S. Zisman, and E. Duek, *Phys. Rev. C* **22**, 1080 (1980).

<sup>8</sup>H. Utsunomiya, T. Nomura, T. Inamura, T. Sugitate, and T. Motobayashi, *Nucl. Phys.* **A334**, 127 (1980).

<sup>9</sup>D. Hilscher, J. R. Birkelund, A. D. Hoover, W. U. Schröder,

- W. W. Wilcke, J. R. Huizenga, A. C. Mignerey, K. L. Wolf, H. F. Breuer, and V. E. Viola, Jr., *Phys. Rev. C* **20**, 576 (1979).
- <sup>10</sup>T. Fukuda, M. Ishihara, H. Ogata, I. Miura, T. Shimoda, K. Katori, S. Shimoura, M. K. Tanaka, E. Takada, and T. Otsuka, *Nucl. Phys.* **A425**, 548 (1984).
- <sup>11</sup>C. Borcea, E. Gierlik, R. Kalpakchieva, Nguyen Hoai Chau, YU.TS. Oganessian, T. Pawlat, and Yu. E. Penionzhkeuch, *Nucl. Phys.* **A415**, 169 (1984).
- <sup>12</sup>R. L. Auble, J. B. Ball, F. E. Bertrand, R. L. Ferguson, C. B. Fulmer, I. Y. Lee, R. L. Robinson, G. R. Young, J. R. Wu, J. C. Wells, and H. Yamada, *Phys. Rev. C* **25**, 2504 (1982).
- <sup>13</sup>D. J. Parker, J. Asher, T. W. Conlon, and I. Naquib, *Phys. Rev. C* **30**, 143 (1984).
- <sup>14</sup>S. L. Tabor, L. C. Dennis, and K. Abdo, *Nucl. Phys.* **A391**, 458 (1982).
- <sup>15</sup>Zhang Li, Jin Gen-ming, Wang Da-yan, Wang Xi-ming, and Zhang Bao-guo, *Proceedings of the Tsukuba International Symposium on H-I Fusion Reaction*, 1984, p. 397.
- <sup>16</sup>Wang Da-yan, Jin Gen-ming, Zhang Li, Yue Hai-kui, and Wang Xi-ming, *Proceedings of the Tsukuba International Symposium on H-I Fusion Reaction*, 1984, p. 399; *Proceedings of the International Conference on Nuclear Physics*, Florence, Italy, 1983, p. 591; *Phys. Energ. Fort. Phys. Nucl.* **10**, 68 (1986).
- <sup>17</sup>Wang Da-yan, Li Zu-yu, Yuan Shuang-gui, Guo Zhong-yan, Jin Gen-ming, Xu Guo-jun, Yue Hai-kui, Wang Xi-ming, Chen Ju-sheng, Zeng Wen-bing, Xie Hong-mei, Qian Zheng-guang, Zhang Li, and Dai Guang-xi, *Phys. Energ. Fort. Phys. Nucl.* **6**, 609 (1982); *Chin. Phys.* **3**, 905 (1984).
- <sup>18</sup>Dai Guang-xi, Jin Gen-ming, Yuan Shuang-gui, Guo Zhong-yan, Zeng Wen-bing, Chen Ju-sheng, Li Zu-yu, Wang Da-yan, and Xu Guo-jun, *Phys. Energ. Fort. Phys. Nucl.* **7**, 86 (1983); *Chin. Phys.* **3**, 912 (1983).
- <sup>19</sup>Zhu Yong-tai, Shen Wen-qing, Qiao Wei-ming, Zhang Zhen, Zhang Yu-hu, Wu En-chiu, Yin Shu-zhi, Zhan Wen-Long, Zheng Zhi-hao, Fan Guo-ying, and Mai He-bing, *Phys. Energ. Fort. Phys. Nucl.* **9**, 447 (1985).
- <sup>20</sup>Xie Yuan-xiang, Wu Guo-hua, Zhu Yong-tai, Miao Rong-zhi, Fong En-pu, Yin xu, Miao He-bing, Cai Jing-xiang, Shen Wen-qing, and Sun Shu-ming, *Phys. Energ. Fort. Phys. Nucl.* **9**, 71 (1985); *Chin. Phys.* **5**, 893 (1985).
- <sup>21</sup>H. Yamada, D. R. Zolnowski, S. E. Cala, A. C. Kahler, J. Pierce, and T. T. Sugihara, *Phys. Rev. Lett.* **43**, 605 (1979).
- <sup>22</sup>T. Nomura, J. Delaunay, C. Tosello, and N. Bendjaballah, *Nucl. Phys.* **A305**, 262 (1978).
- <sup>23</sup>L. Westerberg, D. G. Sarantites, D. C. Hensley, R. A. Dayras, M. L. Halbert, and J. H. Barker, *Phys. Rev. C* **18**, 796 (1978).
- <sup>24</sup>T. Inamura, T. Kojima, T. Nomura, T. Sugitate, and H. Utsumomiya, *Phys. Lett.* **84B**, 71 (1979).
- <sup>25</sup>R. L. Robinson, R. L. Auble, I. Y. Lee, M. J. Martin, G. R. Young, J. Gomezdel, J. Gomezdel Campo, J. B. Ball, F. E. Bertrahd, R. L. Ferguson, C. B. Fulmer, J. R. Wu, J. C. Wells, and H. Yamada, *Phys. Rev. C* **24**, 2084 (1981).
- <sup>26</sup>J. Wilczynski, K. Siwek-Wilczynska, J. Wan Dreiel, S. Gonggrijp, D. C. J. M. Hageman, R. V. F. Janssens, L. Lukasiak, and R. H. Siemssen, *Phys. Rev. Lett.* **45**, 606 (1980); *Nucl. Phys.* **A373**, 109 (1982).
- <sup>27</sup>H. Ho, P. L. Gonthier, G.-Y. Fan, W. Kühn, A. Pfoh, L. Schad, R. Wolski, J. P. Wurm, J. C. Adloff, D. Disdier, A. Kamili, V. Rauch, G. Rudolf, F. Scheibling, and A. Strazzeri, *Phys. Rev. C* **27**, 584 (1983).
- <sup>28</sup>H. Ho, G.-Y. Fan, P. L. Gonthier, W. Kühn, B. Lindl, A. Pfoh, L. Schad, R. Wolski, and J. P. Wurm, *Nucl. Phys.* **A437**, 465 (1985).
- <sup>29</sup>R. K. Bhowmik, J. Van Driel, R. H. Siemssen, G. J. Balster, P. B. Goldhoorn, S. Gonggrijp, Y. Iwasaki, R. V. F. Janssens, H. Sakai, S. Siwek-Wilczynska, and W. A. Sterrenburg, *Nucl. Phys.* **A390**, 117 (1982).
- <sup>30</sup>Jin Gen-ming, Zhang Li, Wang Xi-ming, Wang Da-yan, Yue Hai-kui, and Zhang Bao-guo, *Phys. Energ. Fort. Phys. Nucl.* **9**, 209 (1985); *Chin. Phys.* **6**, 65 (1986).
- <sup>31</sup>K. Siwek-Wilczynska, E. H. Dumarchie, Van Voorthuysen, J. Van Popta, R. H. Siemssen, and J. Wilczynski, *Phys. Rev. Lett.* **42**, 1599 (1979); *Nucl. Phys.* **A330**, 150 (1979).
- <sup>32</sup>C. Gerschel, A. Gillibert, N. Perrin, and T. Tricoire, *Z. Phys.* **A322**, 433 (1985).
- <sup>33</sup>C. Gerschel, *Nucl. Phys.* **A387**, 297 (1982).
- <sup>34</sup>J. P. Wurm, *Proceedings of the International Conference on Nuclear Behavior at High Angular Momentum*, Strasbourg, 1980; *J. Phys. C* **10**, 200 (1980).
- <sup>35</sup>Xu Shu-wei, Wu Guo-hua, Miao Yung-zhi, and Han Fai, *Chin. Phys.* **3**, 646 (1983).
- <sup>36</sup>R. Weiner and M. Weström, *Phys. Rev. Lett.* **34**, 1523 (1975); *Nucl. Phys.* **A286**, 282 (1977).
- <sup>37</sup>H. H. Gutbrod, A. Sandoval, P. J. Johansen, A. M. Poskanzer, J. Gosset, W. G. Meyer, G. D. Westfall, and R. Stock, *Phys. Rev. Lett.* **37**, 667 (1976).
- <sup>38</sup>J. Gosset, H. H. Gutbrod, W. G. Meyer, A. M. Poskanzer, A. Sandoval, R. Stock, and G. D. Westfall, *Phys. Rev. C* **16**, 629 (1977).
- <sup>39</sup>J. J. Griffin, *Phys. Rev. Lett.* **17**, 478 (1966).
- <sup>40</sup>H. Machner, *Phys. Rev. C* **28**, 2173 (1983); E. Holub, D. Hilscher, G. Ingold, U. Jahnke, H. Orf, and H. Rossner, *Phys. Rev. C* **28**, 252 (1983).
- <sup>41</sup>Koji Niita, *Z. Phys. A* **316**, 309 (1984).
- <sup>42</sup>T. Udagawa and T. Tamura, *Phys. Rev. Lett.* **45**, 1311 (1980).
- <sup>43</sup>A. Schwarzschild and C. Zuppanic, *Phys. Rev.* **129**, 854 (1963).
- <sup>44</sup>Nagamiya, M. C. Lemaire, E. Moeller, S. Schnetzer, G. Shapiro, H. Steiner, and I. Tanihata, *Phys. Rev. C* **24**, 971 (1981).
- <sup>45</sup>J. Kasagi, S. Saini, T. C. Awes, G. Galonsky, C. K. Gelbke, G. Poggi, D. K. Scott, K. L. Wolf, and R. L. Legrain, *Phys. Lett.* **B104**, 434 (1981).